ISSN 2075-1133, Inorganic Materials: Applied Research, 2020, Vol. 11, No. 5, pp. 1144–1152. © Pleiades Publishing, Ltd., 2020.
Russian Text © The Author(s), 2020, published in Perspektivnye Materialy, 2020, No. 4, pp. 44–57.

MATERIALS FOR ENSURING HUMAN VITAL ACTIVITY AND ENVIRONMENTAL PROTECTION

Hybrid Tricalcium Phosphate/Hydrogel Constructs Functionalized with an Antitumor Drug for Bone Tissue Regeneration

P. A. Karalkin[a], *, N. S. Sergeyeva[a], I. K. Sviridova[a], V. A. Kirsanova[a], S. A. Akhmedova[a], Ya. D. Shansky[a], N. V. Leontyev[b], D. M. Zuyev[c], E. S. Klimashina[b], P. V. Yevdokimov[b], and V. I. Putlyaev[b]

[a] *Moscow Oncology Research Center, National Medical Research Center of Radiology, Ministry of Health of Russia, Moscow, 125284 Russia*

[b] *Department of Chemistry, Moscow State University, Moscow, 119991 Russia*

[c] *Department of Materials Science, Moscow State University, Moscow, 119991 Russia*

**e-mail: pkaralkin@gmail.com*

Received June 6, 2019; revised June 26, 2019; accepted June 27, 2019

Abstract—Hybrid materials designed for the regeneration of bone defects and consisting of a resorbable ceramic base (tricalcium phosphate, TCP) coated with a layer of hydrophilic biodegradable polymer have been developed. Biocompatibility of the ceramics was evaluated through in vitro tests using cultures of human skin fibroblasts. To increase the therapeutic potential, the created model structures were saturated with the antitumor drug doxorubicin within the composition of the coating of UV-polymerizable hydrogel based on polyacrylamide/polyethylene glycol diacrylate (PAA/PEGDA). The kinetics of drug release was studied by spectrophotometry using saline. The studied hybrid constructs had low cytotoxicity. Saturation of the structures with the antitumor drug resulted in its prolonged release. The results demonstrate the technological feasibility of creating osteoconductive implants based on calcium phosphates suitable for local delivery of antitumor drugs.

Keywords: hybrid biomaterials, tricalcium phosphate, biodegradation, hydrogels, doxorubicin, local drug delivery

DOI: 10.1134/S2075113320050160

INTRODUCTION

Tissue engineering constructs (TECs) are used in regenerative methods of treatment to restore biological functions of the bone. Creation of TECs for the treatment of bone defects is especially important when the size of the defect exceeds the critical level and the body's own capabilities are insufficient to restore bone tissue [1]. TECs are based on biodegradable porous matrices (scaffolds) populated by cells capable of bone formation. In recent years, the problem of targeted delivery of drugs to bone defects as part of TECs has been interdisciplinary as a result of the convergence of regional chemotherapy methods and additive technologies for the manufacture of scaffolds for tissue reconstruction of bone defects of various, including oncological, origin. The very concept of using such functionalized constructions is due to the widespread metastatic damage to bone tissue, the frequency of which reaches 65–75% for breast and prostate cancer, about 60% for thyroid cancer, and up to 40% for cases of lung and kidney cancer in patients with these nosologies [2]. The use of scaffolds filled with antitumor drugs can significantly reduce the likelihood of metastasis of osteosarcoma [3–5].

Such TECs are based on 3D-printed macroporous calcium phosphate ceramics which have an optimal architecture (with regular, interconnected macropores) [6, 7] and contain a cytostatic drug of the anthracycline, platinum, or taxane group. To ensure prolonged local chemotherapy immediately after surgery, it is required to have an additional layer on the surface of TEC to inhibit the release of the drug. Hydrophilic biocompatible polymers, hydrogels capable of swelling, are often used as such a layer [8, 9]. There are various methods of crosslinking in polymer solutions for their gelation [10, 11]. In terms of rheology, hydrogels are viscoelastic bodies capable of sufficiently large (at least 10%) reversible deformations; a viscous element helps relaxing the stresses arising from deformation. This is important for the tight fit of TEC to edges of the bone defect, which is a fundamental requirement for effective osseointegration of the implant. In this work, we used polyacrylamide (PAA) hydrogels crosslinked with polyethylene glycol diacrylate (PEGDA) during photopolymerization. A layer of hydrogel was

Table 1. The composition of the obtained hydrogels based on AA and PEGDA

Properties	Composition no.					
	1	2	3	4	5	6
PEGDA content in gel, ω, wt %	0.625	1.00	2.00	5.00	1.00	35.00
m_{AA}, g	2	2	2	2	2	2
m_{PEGDA}, g	0.0125	0.02	0.05	0.1	0.2	0.7
$m_{photoinitiator}$, g	0.0201	0.0202	0.0205	0.0210	0.0220	0.0270
N_{AA}/N_{PEGDA}	1576	985	394	197	98	28

deposited on the surface of tricalcium phosphate ceramic, β-$Ca_3(PO_4)_2$ (TCP). The ceramic and/or hydrogel layer were filled with a cytostatic drug from the anthracycline antibiotic group, doxorubicin (8S-cis)-10-[(3-amino-2,3,6-trideoxy-α-L-lyxo-hexopyranosyl)oxy]-7,8,9,10-tetrahydro-6,8,11-trihydroxy-8-(hydroxyacetyl)-1-methoxynaphthacene-5,12-dione hydrochloride.

The aim of this work is to develop techniques for fabricating cytostatic-filled TECs on model structures with a flat TCP-ceramic/hydrogel interface and to investigate the kinetics of drug release from these structures.

MATERIALS AND METHODS

Obtaining β-TCP Tablets

TCP ceramic was obtained in the form of tablets with a diameter of 6 mm and mass of 100–105 mg by pressing β-TCP powder (chemically pure) in acetone for 1.5 min at a pressure of 3 atm. Sintering was carried out in a muffle furnace at 1100°C for 6 h. At the end of sintering, the following parameters of ceramic tablets were measured: mass, diameter, and height.

Precipitation of Carbonate Hydroxyapatite (CHA) on β-TCP Tablets from a Simulated Body Fluid (SBF)

In order to obtain bioactive coatings on the surface of β-TCP tablets, CHA was precipitated during thermostating in 5×SBF for seven days at 37°C. After seven days, the tablets were separated from the solution, washed with ammonia solution (pH 10–11), and placed in a drying chamber at 60°C for one day.

Hydrogel Layer Application

The organic component of the used composite consisted of a hydrogel based on acrylamide (AA) and polyethylene glycol diacrylate (PEGDA) with a molar mass of 700 g/mol. To obtain such gels, 2 g of acrylamide powder was dissolved in 8 g of saline (0.9% aqueous sodium chloride solution) while stirring. Then six gels of different compositions were obtained (Table 1) by adding the corresponding volume of PEGDA (density 1.12 g/mL at 25°C) to the existing solution.

The amount of APi-180 photoinitiator (2-hydroxy-1-[3-(hydroxymethyl)phenyl]-2-methyl-1-propanone) added to each specific gel composition was calculated as 1% of the total mass of the organic component. Figure 1 shows the sequence of operations. In some experiments, the hydrogels were dried in air at room temperature and in a sublimator, followed by cycles of swelling in saline.

X-ray Phase Analysis (XRD)

Qualitative X-ray phase analysis was carried out using a Rigaku D/Max-2500 rotating anode diffrac-

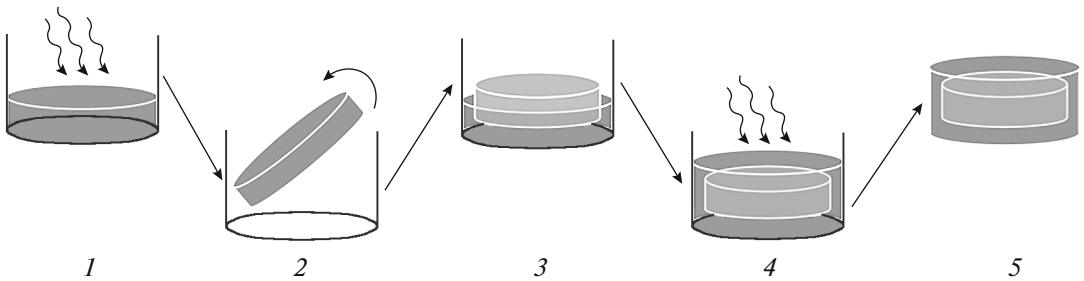

Fig. 1. Stages of coating the TCP tablets with hydrogels: (*1*) introducing 50 μL of a gel solution into a well of a plate and initiating its irradiation; (*2*) turning over a partially polymerized gel; (*3*) adding the TCP tablet; (*4*) adding 50 μL of gel and re-irradiation; (*5*) removing the gel-coated tablet from the well and placing it onto a glass slide, followed by exposure under a UV source until polymerization is complete.

tometer (Japan). The diffraction patterns were recorded in reflection mode (Bragg-Brentano geometry) using CuK_{av} radiation in quartz cells without rotation averaging. XRD parameters: range of angles 2θ = 3°–70° in steps of $2\theta \sim 0.02°$, spectrum detection rate 5°/min. For spectrum correction, silicon powder (ASTM) was used as an internal standard. Qualitative analysis of the obtained X-ray diffraction patterns was carried out in the WinXPOW software program using the ICDD PDF-2 database.

Scanning Electron Microscopy (SEM)

The microstructures of the samples were examined using a LEO SUPRA 50VP field emission scanning electron microscope (Carl Zeiss, Germany), as well as a FIB NVision 40 electron microscope (Carl Zeiss, Germany). For this purpose, a layer of carbon or chromium was deposited on the samples (QT-150T ES sputter coater, Quorum Technologies, United Kingdom). The accelerating voltage of the electron gun was 3–10 kV. Images were obtained at magnifications up to ×100000 using a type II secondary electron (SE2) detector.

Investigation of the Kinetics of Drug Release

Two types of experimental conditions were used: (a) static conditions at 25°C, that is, the structure saturated with hydrogel was always in a constant volume of saline solution; (b) dynamic conditions at 37°C, the saline solution was changed after each measurement.

(a) Static conditions. Previously dried samples were placed in sealed beakers, one sample per beaker containing 8 mL of saline. The absorption spectrum of the doxorubicin released into the solution was measured at several time points: 0, 2, 4, 6, 8, 10, 25, 50, 100, and 200 min. Before each measurement, the solution in the beaker was mixed and using an automatic pipette 3 mL was transferred into a quartz cuvette 1 cm wide. After the measurement, the doxorubicin solution was transferred from the cuvette using the same pipette back into the beaker and hermetically sealed until the next measurement. In some experiments, the solution was diluted 6-fold before spectrophotometry.

(b) Dynamic conditions. Two methods of introducing the drug into the construct were employed: (1) a ceramic tablet was impregnated with a layer of doxorubicin, and then a layer of hydrogel was applied to the tablet; (2) a layer of hydrogel was applied to the tablet and dried, and then the hydrogel swelled in a solution of doxorubicin (similar to experiments under static conditions). A ceramic tablet impregnated with a solution of doxorubicin was sometimes used as a reference sample. The constructs were placed in containers with 3 mL of saline at 37°C; after measurement, new saline was poured into the container.

(c) Preparation of standard solutions. First, 0.12 g of doxorubicin (TEVA) was dissolved in 25 mL of saline and stirred until the precipitate was completely dissolved. Then 0.125, 0.2, 0.25, 0.375, 0.5, 1, 1.25, 2.5, and 5 mL of the obtained standard solution were added to nine measuring containers, after which saline was used to bring the volume to 10 mL. For analysis and calculation of a calibration curve, the solutions were transferred to quartz cuvettes with an optical path length of 1 cm, and spectrophotometry was carried out in the wavelength range of 300–800 nm (UV and visible spectrum) using a PerkinElmer Lambda 35 spectrophotometer.

(d) Spectrophotometric analysis of solutions. The measurement procedure was partially described above. In another series of experiments, similar operations were carried out up to a time point of 10 min inclusive. Starting from the 25th minute, 500 μL of doxorubicin solution was taken from the beaker and transferred to a clean container, adding 2500 μL of saline, followed by spectrophotometric measurement. The concentration of the drug released into the solution was calculated at the wavelength of its maximum absorption.

Investigation of the Cytotoxicity of Hybrid Materials

The cytotoxicity of the resulting hybrid structures consisting of TCP coated with a layer of CHA and/or hydrogel was evaluated in accordance with GOST ISO 10993-5-2011 [12]. The study was carried out on a transplanted line of immortalized human skin fibroblasts (HFs, strain 1680h TERT, Engelhardt Institute of Molecular Biology, Russian Academy of Sciences). For cultivation, we used DMEM growth medium, 10% fetal calf serum (Gibco, United States), 60 mg/mL L-glutamine, 50 μg/mL gentamicin, and 20 mM HEPES solution. To prepare extracts from the test samples, they were placed in glass vials, five samples per vial, with a total surface area of 3.54 cm^2, followed by addition of 1.2 mL of a nutrient medium. Extraction was carried out at 37°C in a thermostat with constant stirring on a horizontal orbital shaker for 24 h. The density of HF cells in the experiment was 5×10^3 cells in each well of a 96-well plate in 200 μL of nutrient medium. After 3.5 h of HF inoculation, the growth medium was removed from each well and 100.0 μL of material extracts were added. As negative and positive controls of cytotoxicity, we used a nutrient medium and a medium containing 50 wt % dimethyl sulfoxide (DMSO), respectively. The cytotoxic effect of the extracts on HFs was evaluated by the MTT test after 24-h incubation. To calculate the final indicators of cell survival, the percentage of viable cells in the presence of a pure nutrient medium was taken as 100%.

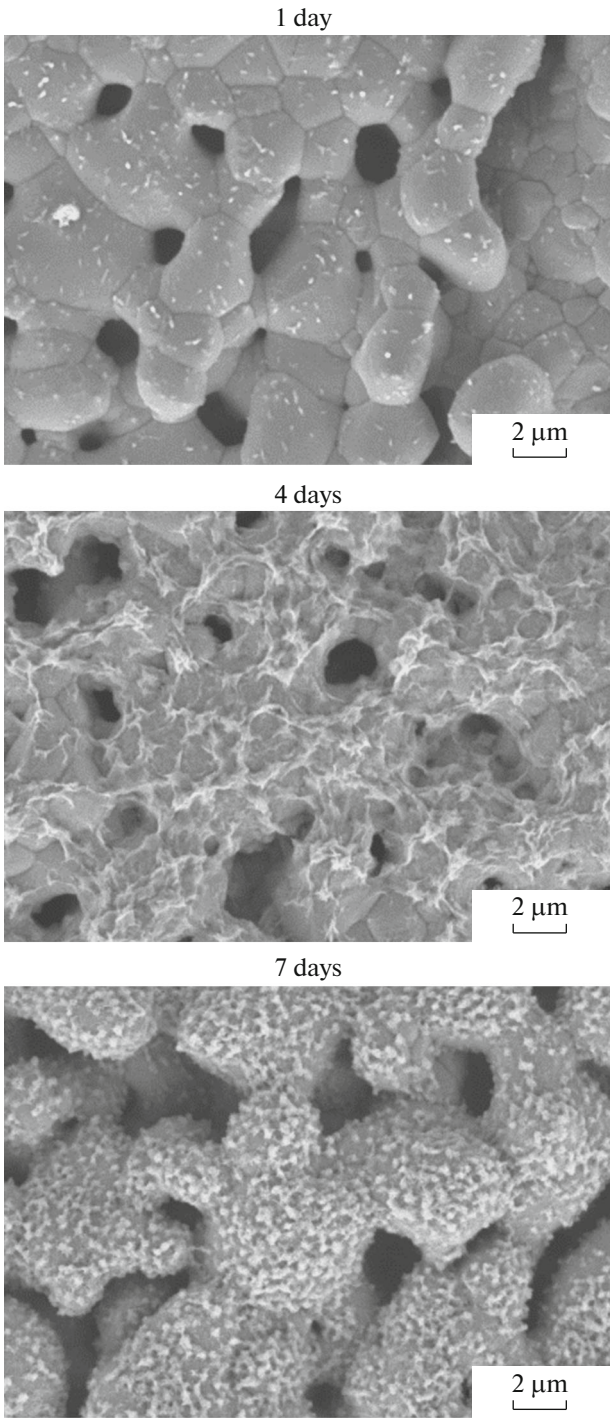

Fig. 2. Microstructure of ceramic made of TCP aged in a 5×SBF solution (the exposure time is given below the pictures); accumulation of CHA crystals on the ceramic surface is visible.

Statistical Processing of Results

Statistical analysis of the data was carried out using STATISTICA ver. 10.0 software (2011, StatSoft, Inc., United States) and Microsoft Excel 365. For the majority of the studied parameters, we calculated the average and standard deviation.

RESULTS AND DISCUSSION

Two methods have been tested for the synthesis of TCP and TCP/hydroxyapatite (HA, $Ca_{10}(PO_4)_6(OH)_2$) powders with the required granulometry (d_{50} at a level of 1 μm): (a) solid-phase synthesis from $CaCO_3$ and $Ca_2P_2O_7$ (obtained by thermolysis of brushite precipitated from aqueous solutions) at 950°C; (b) precipitation of hydrated tricalcium phosphate $Ca_3(PO_4)_2 \cdot xH_2O$—amorphous calcium phosphate (ACP) or nonstoichiometric HA (nHA) $Ca_{10-x}(HPO_4)_x(PO_4)_{6-x}(OH)_{2-x}$ with a reaction pathway given by x (X = NO_3, CH3COOCl):

$$\begin{aligned} &Ca(X)_2 + (NH_4)_2HPO_4 + NH_4OH \\ &\quad = Ca_3(PO_4)_2 \cdot xH_2O\downarrow \\ &\times (Ca_{10-x}(HPO_4)_x(PO_4)_{6-x}(OH)_{2-x} + 6NH_4X. \end{aligned} \quad (1)$$

It should be noted that all three types of synthesis make it possible to obtain powders for the fabrication of TCP and TCP/HA ceramics with the required characteristics. The disadvantages of solid-phase synthesis include the larger particle size and nonstoichiometry of the initial mixture, which is sometimes observed in IR spectra (fluctuations of the P_2O_7 groups). Synthesis through ACP is complicated and results in aggregated powders with high water content and high shrinkage during sintering. Thus, solid-phase synthesis and nHA deposition turn out to be acceptable for obtaining model (flat geometry) and macroporous ceramic from TCP and TCP/HA. The solid-phase synthesis TCP powder after disaggregation in a ball planetary mill in an acetone liquid medium with the addition of a surfactant (Triton X-100) for 1 h has a distribution with an average particle size of ~2 ± 0.5 μm. The obtained solid-state synthesis powders were used to obtain ceramic with 15–20% porosity (Fig. 2; in some experiments, porosity was adjusted to 30% by etching the ceramic with citric acid) by sintering at 1100°C for 6 h. The ceramic was used to fabricate 2-layer (TCP tablet coated with a layer of hydrogel) and 3-layer (TCP tablet coated with a layer of CHA deposited from 5×SBF, a hydrogel layer on top of CHA) TECs.

Figure 3 shows dependences of the polymerization depth of photocurable hydrogels on the radiation dose when using different PEGDA contents. An increase in PEGDA content to 2.5 wt % results in a slight decrease in the critical polymerization energy (Table 2), while the use of 5% PEGDA makes it possible to increase the reactivity of the composition to obtain PAA-PEGDA-hydrogel. To increase the reactivity, that is, the possibility of applying thin layers of PAA-PEGDA-hydrogel coating, it is necessary either to increase the concentration of PEGDA, which will

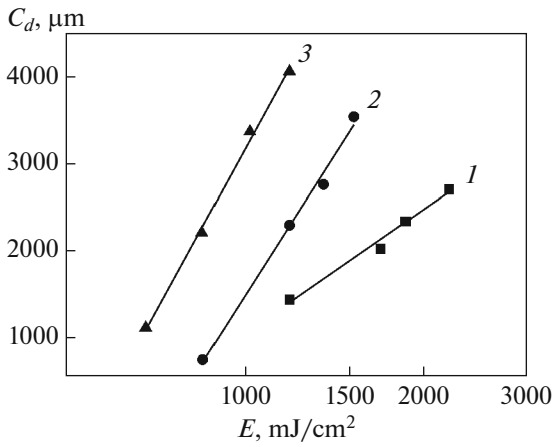

Fig. 3. Dependence of the polymerization depth on the radiation dose when using different PEGDA contents to obtain photocurable PAA-PEGDA hydrogels: (*1*) 0.625; (*2*) 2.5; (*3*) 5%.

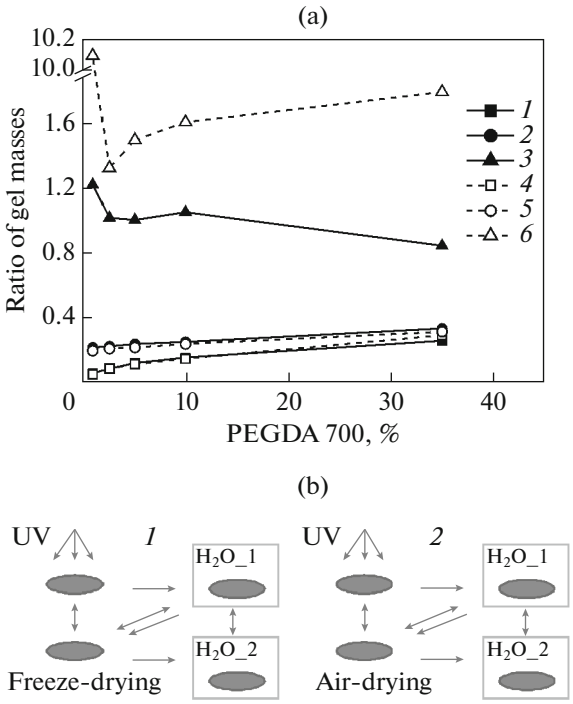

Fig. 4. (a) The relative change in the mass of hydrogels after different sequences of operations: (*1*) after freeze-drying/in water before drying; (*2*) after freeze-drying/after UV exposure; (*3*) in water after freeze-drying/in water after UV exposure; (*4*) after drying in air/in water after drying in air; (*5*) after drying in air/after UV exposure; (*6*) in water after drying in air/in water after UV exposure. (b) The sequence diagram of operations of UV polymerization, drying (in air or sublimation), hydration, and rehydration.

result in damage to the applied layer owing to higher fragility of the gels, or to increase the amount of photoinitiator, which in turn can reduce the biocompatibility of the coatings.

Nevertheless, the results of biocompatibility testing in our experiments (Table 3) suggested that there was no pronounced cytotoxicity in the used compositions of ceramic materials and hydrogel coatings. The percentage of viable human skin fibroblasts after 24 h of cultivation in the presence of extracts from hybrid materials of various compositions was, on average, at least 80%.

The processes of drying and swelling of hydrogels are most strongly affected by the freeze-drying of water-swollen gel (increased subsequent swelling) (Fig. 4). Two compositions with 0.625 and 35% PEGDA with irreversible drying-swelling can be distinguished, that is, weakly and very strongly crosslinked gels. The microstructure of the gels after freeze-drying (Fig. 5) is characterized by varying degrees of structuredness. Strongly crosslinked gels are the most structured; however, in the range of average concentrations of a crosslinking agent (for example, 5% PEGDA), the gel appears unexpectedly dense; at the same time, low concentrations of a crosslinking agent (0.625–2.5%) result in both dense and netted sections; that is, gels are less uniform. Gels with PEGDA content higher than 5% were quite fragile; for this reason the gel often peeled off from the TCP tablet or the gel layer was destroyed. At the same time, gels with PEGDA content of less than 1% with prolonged swelling in saline or DMEM at 37°C degraded irreversibly after 1 day. Taking into account the behavior during swelling, strength, and adhesion of the gel layer, for further studies, we decided to use PAA/PEGDA hydrogels with PEGDA contents of 2.5 and 5%. The LC_{50} value for the APi-180 photoinitiator is 8.7 mmol/L or 1.6898 g/L [13]; therefore, for in vitro applications, the use of hydrogels with the photoinitiator content higher than this concentration is highly undesirable. For the obtained compositions, the APi-180 content did not exceed 0.38 g/L (1% relative to the PAA content), which suggests relative safety of their use in tissue engineering.

The red color of doxorubicin, when introduced into TEC, has both a positive side (when using spectroscopic methods for analysis) and a negative side

Table 2. Data on the critical polymerization energy and photosensitivity of compositions with different PEGDA contents used to produce photocurable PAA-PEGDA hydrogels

PEGDA content, %	Critical polymerization energies, E_c, mJ/cm^2	Photosensitivity, D_p, μm
0.625	756	2733 ± 519
2.5	726	4624 ± 273
5	555	5381 ± 248

Table 3. Results of acute cytotoxicity testing of extracts from ceramic disks of TCP, additionally coated with a layer of CHA and/or hydrogel based on PEGDA/AA

Sample series no.	Composition	Viable cell population, VCP, %	Cytotoxicity index, %
1	Culture medium (negative cytotoxicity control)	100	0
2	TCP	90.9	9.1
3	TCP + CHA layer	81.3	18.7
4	TCP + 2.5% PEGDA/AA	81.6	18.4
5	TCP + CHA layer + 2.5% PEGDA/AA	81.6	18.4
6	TCP + 5% PEGDA/AA	79.8	20.2
7	TCP + CHA layer + 5% PEGDA/AA	78.1	21.9
8	Culture medium with 50% DMSO (dimethyl sulfoxide) (positive cytotoxicity control)	4.6	95.4

(the absorption maximum of about 480 nm falls into the absorption band of the photoinitiator). On the basis of the obtained absorption spectra, we determined the wavelength at which the detected optical density of doxorubicin hydrochloride is maximal, 480 nm. After that, we calculated a calibration dependence to determine the concentration of doxorubicin at a given wavelength. Starting with optical density of 2.5, the absorption curves show noise (Fig. 6a) primarily due to the insufficient sensitivity of the device (spectrophotometer PerkinElmer Lambda 35) for detecting low-intensity radiation transmitted through a highly absorbing solution. To avoid large systematic negative errors, it was decided to calculate a calibration function at an absorption wavelength of 400 nm. The data obtained at a wavelength of 480 nm were approximated to a straight line defined by the equation

$$y = (15.9 \pm 1.1)c + (0.30 \pm 0.09),$$
$$(P = 0.95,\ n = 8,\ r = 0.98043), \quad (2)$$

where c is the concentration of doxorubicin hydrochloride, mg/mL; P is the confidence probability; n is the number of points; and r is the correlation coefficient. For a wavelength of 400 nm, the corresponding dependence has the form

$$y = (4.8 \pm 0.1)c + (0.06 \pm 0.01),$$
$$(P = 0.95,\ n = 8,\ r = 0.99781). \quad (3)$$

At both the wavelengths, the lower PEGDA content in the gel and the lower crosslink density resulted in a greater amount of doxorubicin transferred to the external solution. After 100 min from the moment the samples were placed in saline, the kinetic curve (especially for weakly crosslinked gels) almost plateaued. The diffusion rate of the drug from the gel into the external solution decreased, which can be explained by the fact that the solution approached the saturation state. Thus, the lower PEGDA content in the gel corresponded to the rapid release of the drug from the samples (as can be seen from Figs. 6b and 6c, this tendency can be observed in photometry at both wavelengths). Such, at first glance, unexpected behavior may be the result of nonchemical saturation of the samples with doxorubicin, that is, the penetration of the drug into the hydrogel during its physical swelling. The loosely entangled molecular network inherent in less crosslinked hydrogels absorbed a larger volume of the drug solution, providing a natural decrease in the concentration of released doxorubicin from the first composition to the fourth. On the other hand, the low structuredness slowed the diffusion of molecules from the hydrogel layer into the solution owing to mechanical difficulties. For this reason, doxorubicin was released longer from less crosslinked gels, which corresponds to the growing proportion of drug release from the first composition to the fourth.

Under dynamic conditions, the kinetic curves of doxorubicin release (Figs. 7a and 7b) from structures with the gel layer containing different amounts of the PEGDA crosslinking agent reveal the previously observed trends. The less crosslinked and, therefore, stronger swelling gel (Fig. 7c) slows down the release of the drug in comparison with the stronger crosslinked gels. It should be noted that stronger sorption and, accordingly, weaker release by strongly swelling gels were noted in the literature earlier. This is explained by several reasons: (a) the specific poorly organized structure of weakly crosslinked gels, (b) the osmotic flow of the solvent directed into the gel, and (c) the alignment of the concentration of the drug in a highly swelling gel and a surrounding solution.

Let us note that, in a situation where the gel acts as a diffusion-inhibiting layer (Fig. 7b) and the drug is within a ceramic tablet, the presence of the gel layer does not affect the release rate too much, although this rate decreases markedly when the drug is initially in the gel layer (Fig. 7a). Thus, the limiting stage here is the release of the drug from phosphate ceramic. Visually, the tablets remain stained red even after a two-week experiment. This suggests the presence of specific sorption of doxorubicin on TCP (apparently,

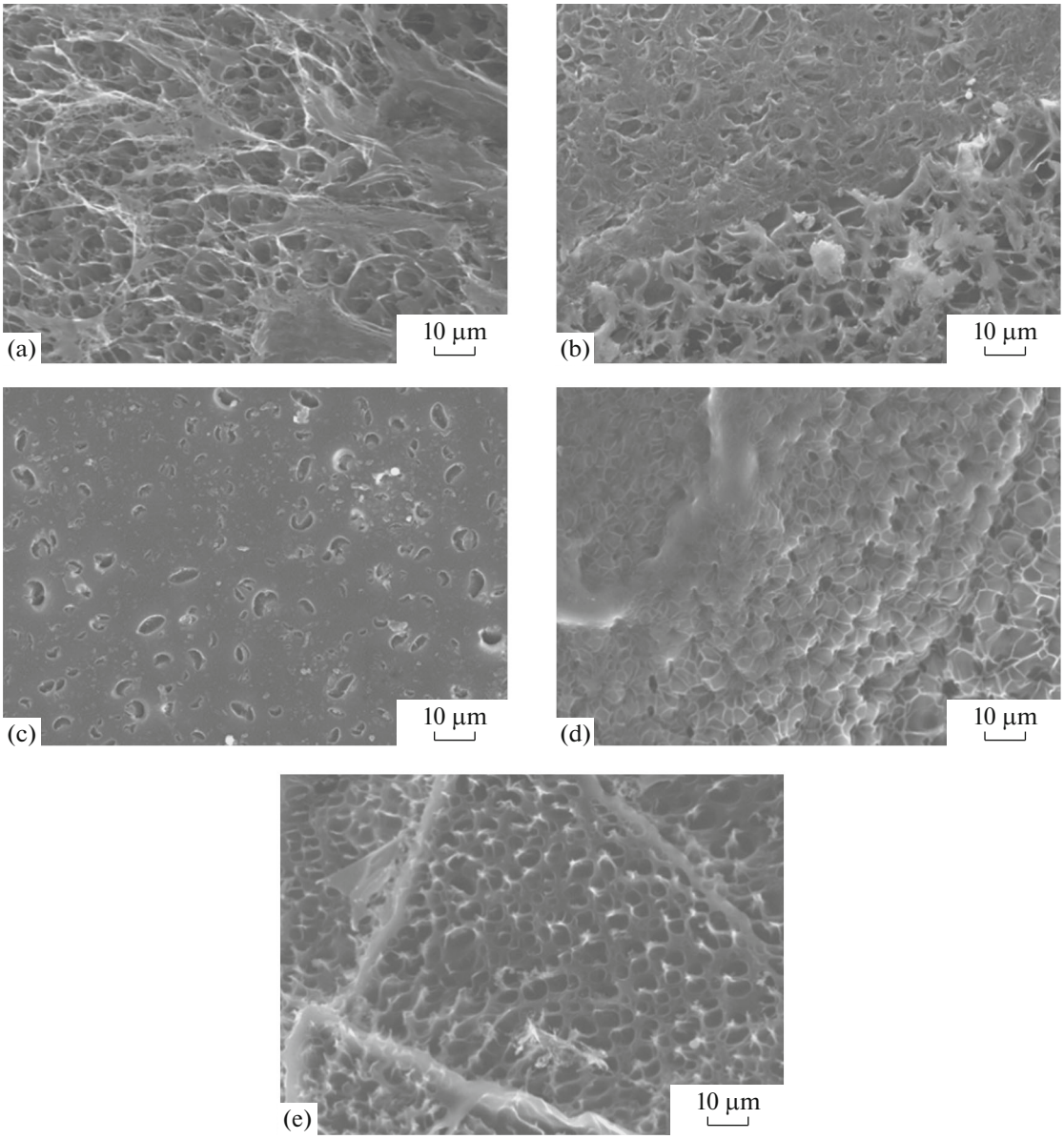

Fig. 5. The microstructure of the gels after freeze-drying with different PEGDA contents: (a) 1; (b) 2.5; (c) 5; (d) 10; (e) 35%.

chemisorption). If a solution containing more than 50 mM phosphate is added to a doxorubicin solution in water, one would observe a coarse-fibrous red precipitate (apparently, doxorubicin hydrophosphate). Such a fact has not been reflected in the literature, although it is being rather actively discussed privately by researchers working with this drug.

In general, the release of the drug from the fabricated structures is characterized by a rapid stage that lasts up to 10 h, during which the release ranges from 10% (when the drug is placed in ceramic) to 60% (the drug is in a weakly crosslinked gel layer). This is followed by a slow release stage, the duration of which is determined either by the complete degradation of the gel (several days at the crosslinking level of 1%) or by resorption of TCP (at least six months).

CONCLUSIONS

Model hybrid tissue-engineering constructions designed for the regeneration of bone defects and consisting of a resorbable ceramic base (TCP) coated with a layer of hydrophilic biodegradable polymer have been developed.

Biocompatibility of the ceramics was evaluated through in vitro tests using human fibroblast cell cultures.

To increase the therapeutic potential, the created model structures were saturated with the anti-

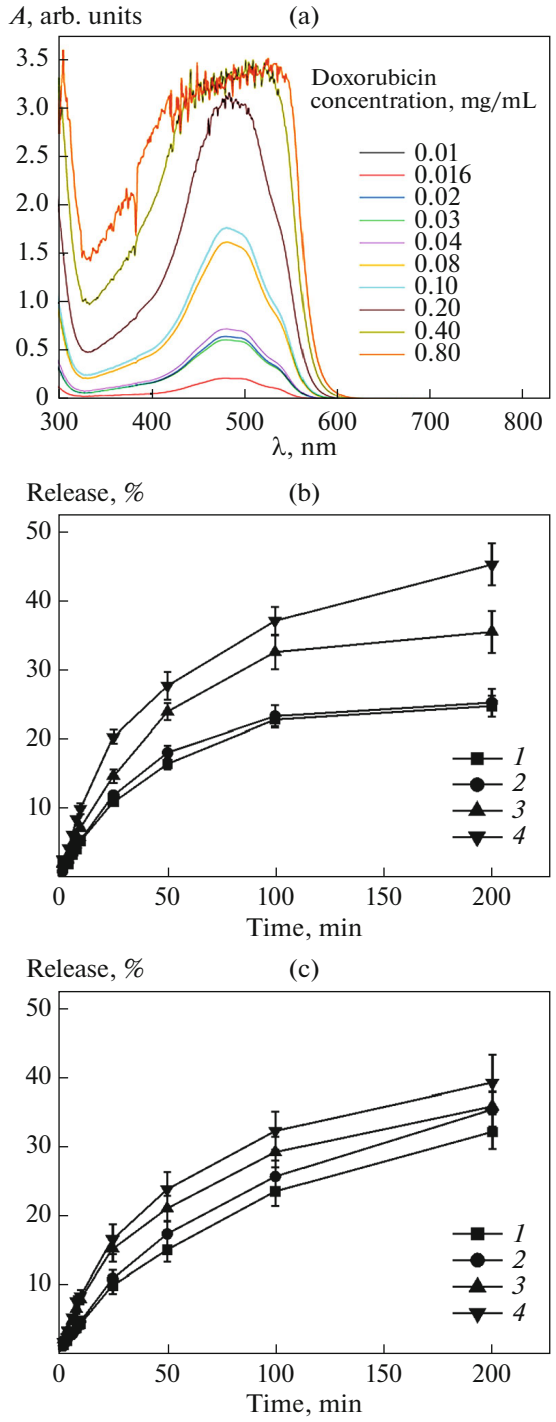

Fig. 6. (a) UV/Vis spectra of doxorubicin solutions; (b, c) kinetic curves of doxorubicin release (the method of injecting the drug into the construct: the dried gel swelled in a solution of doxorubicin) at 25°C; PEGDA content, see Table 1, obtained at (b) 400 nm and (c) 480 nm. (*1*–*4*) Samples 1–4.

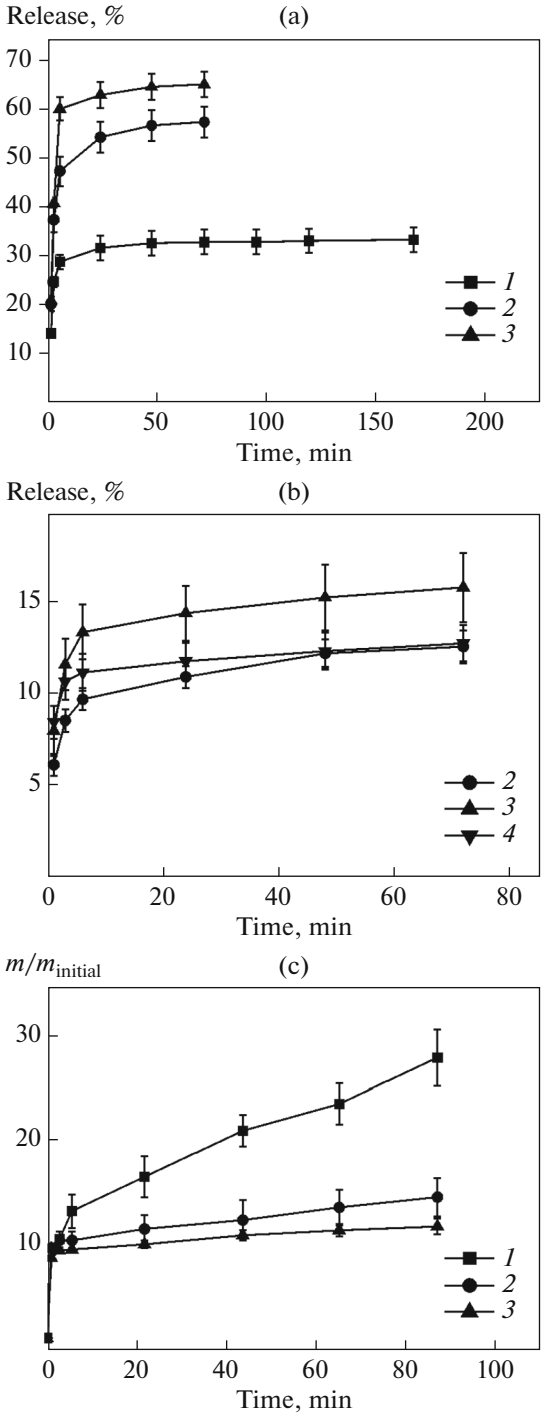

Fig. 7. Kinetic curves of doxorubicin release from constructs with different PEGDA contents in the gel (wt %: (*1*) 0.625; (*2*) 2.5; (*3*) 5; (*4*) tablet) under dynamic conditions at 37°C: (a) the route of administration: doxorubicin in the gel; (b) the route of administration: doxorubicin in a ceramic tablet; (c) swelling of the gels.

tumor drug doxorubicin within the composition of the coating of UV-polymerizable hydrogel based on polyacrylamide/polyethylene glycol diacrylate (PAA/PEGDA).

The kinetics of drug release was studied by spectrophotometry using solutions simulating physiological fluids of the extracellular medium of the body. The studied hybrid constructs had low cytotoxicity. The

drug release from the fabricated structures was characterized by a fast stage lasting up to 10 h, during which from 10% (when placing the drug in ceramic) to 60% (the drug in a weakly crosslinked gel layer) of the drug was released. This was followed by a slow release stage, the duration of which was determined either by the complete degradation of the gel or the resorption of TCP.

These results demonstrate the technological feasibility of creating functionalized osteoconductive implants based on calcium phosphates for local delivery of antitumor drugs.

FUNDING

This work was carried out within the framework of the Russian Foundation of Basic Research grant 18-29-11070_mk using the equipment purchased as part of the Moscow University Development Program.

COMPLIANCE WITH ETHICAL STANDARDS

The authors declare that they have no conflict of interest. This article does not contain any studies involving animals or human participants performed by any of the authors.

REFERENCES

1. Porter, J.R., Ruckh, T.T., and Popat, K.C., Bone tissue engineering: a review in bone biomimetics and drug delivery strategies, *Biotechnol. Prog.*, 2009, vol. 25, pp. 1539–1560.
2. Kaprin, A.D., Starinskii, V.V., and Petrova, G.V., *Zlokachestvennye novoobrazovaniya v Rossii v 2015 godu (zabolevaemost' i smertnost')* (Rate of Malignant Neoplasms in Russia in 2015: Morbidity and Mortality), Moscow: Mosk. Nauchno-Issled. Onkol. Inst. im. A. Gertsena, 2017.
3. Gdowski, A.S., Ranjan, A., and Vishwanatha, J.K., Current concepts in bone metastasis, contemporary therapeutic strategies and ongoing clinical trials, *J. Exp. Clin. Cancer Res.*, 2017, vol. 36, no. 1, p. 108.
4. Miura, S., Mii, Y., Miyauchi, Y., et al., Efficacy of slow-releasing anticancer drug delivery systems on transplantable osteosarcomas in rats, *Jpn. J. Clin. Oncol.*, 1995, vol. 25, no. 3, pp. 61–71.
5. Shishatskaya, E.I., Goreva, A.V., Kuzmina, A.M., Study of the efficiency of doxorubicin deposited in microparticles from resorbable Bioplastotane™ on laboratory animals with Ehrlich's solid carcinoma, *Bull. Exp. Biol. Med.*, 2013, vol. 154, no. 6, pp. 773–777.
6. Ievlev, V.M., Putlyaev, V.I., Safronova, T.V., and Evdokimov, P.V., Additive technologies for making highly permeable inorganic materials with tailored morphological architectonics for medicine, *Inorg. Mater.*, 2015, vol. 51, no. 13, pp. 1295–1313.
7. Putlyaev, V.I., Yevdokimov, P.V., Mamonov, S.A., Zorin, V.N., Klimashina, E.S., Rodin, I.A., Safronova, T.V., and Garshev, A.V., Stereolithographic 3D printing of bioceramic scaffolds of a given shape and architecture for bone tissue regeneration, *Inorg. Mater.: Appl. Res.*, 2019, vol. 10, no. 5, pp. 1101–1108.
8. Kargupta, R., Bok, S., Darr, C.M., Crist, B.D., Gangopadhyay, K., Gangopadhyay, S., and Sengupta, S., Coatings and surface modifications imparting antimicrobial activity to orthopedic implants, *WIREs Nanomed. Nanobiotechnol.*, 2014, vol. 6, pp. 475–495.
9. Bronich, T.K., Polymeric nanogels as new biomaterials for delivering of anticancer drugs, *Vestn. Kazan. Gos. Tekhnol. Univ.*, 2014, vol. 17, no. 3, pp. 175–178.
10. Sivashanmugam, A., Arun Kumar, R., Visnu Priya, M., et al., An overview of injectable polymeric hydrogels for tissue engineering, *Eur. Polym. J.*, 2015, vol. 72, pp. 543–565.
11. Kumar, A., Madhusudana Rao, K., and Han, S.S., Synthesis of mechanically stiff and bioactive hybrid hydrogels for bone tissue engineering applications, *Chem. Eng. J.*, 2017, vol. 317, pp. 119–131.
12. *GOST (State Standard) ISO 10993-5-2011: Medical Devices, Biological Evaluation of Medical Devices, Part 5: Tests for in Vitro Cytotoxicity*, Moscow: Standartinform, 2014.
13. Benedikt, S., Wang, J., Markovic, M., Moszner, N., Dietliker, K., Ovsianikov, A., Grützmacher, H., and Liska, R., Highly efficient water-soluble visible light photoinitiators, *J. Polym. Sci., Part A: Polym. Chem.*, 2016, vol. 54, pp. 473–479.

Translated by K. Lazarev